



HAL
open science

Going live: a comparative analysis of the suitability of the RFP derivatives RedStar, mCherry and tdTomato for intravital and in vitro live imaging of Plasmodium parasites

Stefanie Graewe, Silke Retzlaff, Nicole Struck, Chris Janse, Volker Heussler

► To cite this version:

Stefanie Graewe, Silke Retzlaff, Nicole Struck, Chris Janse, Volker Heussler. Going live: a comparative analysis of the suitability of the RFP derivatives RedStar, mCherry and tdTomato for intravital and in vitro live imaging of Plasmodium parasites. *Biotechnology Journal*, 2009, 4 (7), pp.895. 10.1002/biot.200900035 . hal-00488421

HAL Id: hal-00488421

<https://hal.science/hal-00488421>

Submitted on 2 Jun 2010

HAL is a multi-disciplinary open access archive for the deposit and dissemination of scientific research documents, whether they are published or not. The documents may come from teaching and research institutions in France or abroad, or from public or private research centers.

L'archive ouverte pluridisciplinaire **HAL**, est destinée au dépôt et à la diffusion de documents scientifiques de niveau recherche, publiés ou non, émanant des établissements d'enseignement et de recherche français ou étrangers, des laboratoires publics ou privés.

Going live: a comparative analysis of the suitability of the RFP derivatives RedStar, mCherry and tdTomato for intravital and in vitro live imaging of Plasmodium parasites

Journal:	<i>Biotechnology Journal</i>
Manuscript ID:	biot.200900035.R1
Wiley - Manuscript type:	Technical Report
Date Submitted by the Author:	30-Apr-2009
Complete List of Authors:	Graewe, Stefanie; Bernhard Nocht Institute for Tropical Medicine, Molecular Parasitology Retzlaff, Silke; Bernhard Nocht Institute for Tropical Medicine, Molecular Parasitology Struck, Nicole; Bernhard Nocht Institute for Tropical Medicine, Molecular Parasitology Janse, Chris; Leiden University Medical Center (LUMC, L4-Q), Parasitology, Center of Infectious Diseases Heussler, Volker; Bernhard Nocht Institut for Tropical Medicine, Molecular Parasitology
Keywords:	mCherry, in vitro live imaging, intravital imaging, Plasmodium, RedStar

1
2
3
4
5
6 **Technical Report ((5477 words))**

7
8 **Going live: a comparative analysis of the suitability of the RFP derivatives**
9
10 **RedStar, mCherry and tdTomato for intravital and *in vitro* live imaging of**
11 ***Plasmodium* parasites**
12
13

14
15
16
17 Stefanie Graewe¹, Silke Retzlaff¹, Nicole Struck¹, Chris J. Janse² and Volker T.
18 Heussler¹
19

20
21
22 ¹Department of Parasitology, Bernhard Nocht Institute for Tropical Medicine,
23 Hamburg, Germany
24

25
26
27 ²Leiden University Medical Center, Leiden, The Netherlands
28

29
30
31 *Keywords:* RedStar, mCherry, tdTomato, *in vitro* live imaging, intravital
32 imaging, photobleaching, *Plasmodium*
33

34
35
36
37
38
39 *Corresponding author:* PD Dr. Volker Heussler, Bernhard-Nocht-Strasse 74,
40 20359 Hamburg, Germany, Phone: 0049 40 42818 485, Fax: 0049 40 42818
41 512, Email: heussler@bni-hamburg.de
42
43
44
45
46
47

48 FP fluorescent protein

49 GFP green fluorescent protein

50 MFI mean fluorescence intensity

51 P Plasmodium

RFP red fluorescent protein

Abstract

Fluorescent proteins have proven to be important tools for *in vitro* live imaging of parasites and for imaging of parasites within the living host by intravital microscopy. We observed that a red-fluorescent transgenic malaria parasite of rodents, *Plasmodium berghei*-RedStar, is suitable for *in vitro* live imaging experiments but bleaches rapidly upon illumination in intravital imaging experiments using mice. Therefore, we have generated two additional transgenic parasite lines expressing the novel red-fluorescent proteins tdTomato and mCherry, which have been reported to be much more photostable than first- and second-generation red fluorescent proteins including RedStar. We have compared all three red fluorescent parasite lines for their use in *in vitro* live and intravital imaging of *P. berghei* blood and liver parasite stages, using both confocal and wide-field microscopy. While tdTomato bleached almost as rapidly as RedStar, mCherry showed improved photostability and was bright in all experiments performed.

1 Introduction

The first fluorescent protein to be employed for live imaging experiments was the green fluorescent protein (GFP) from the jellyfish *Aequorea victoria* in 1994 [1]. Shortly after, the red fluorescent protein (RFP) DsRed was discovered in the coral *Discosoma sp.* and subsequently made available for transgenic expression in various other cell types including mammalian cells and parasites [2]. Numerous derivatives of RFP were created, such as the smaller, monomeric variant mRFP1 [3] or the fast-fluorescing RedStar [4]. Since there are many GFP-expressing cell lines and mouse strains, these RFP derivatives are extremely useful for the analysis of interactions between parasites and their hosts [5-8]. We study the development of the *Plasmodium* parasite, the causative agent of malaria, in the mammalian host. An infection of the mammalian host begins after a bite of an infected *Anopheles* mosquito. During the blood meal, sporozoites, that are present in the salivary gland of the mosquito, are injected into the dermis of the mammalian host. They subsequently enter blood vessels [9, 10] and travel through them to the liver, where they invade hepatocytes and develop into thousands of daughter cells, the merozoites. Merosomes, small vesicles filled with merozoites, bud from the infected hepatocyte and are released into the blood stream [8, 11, 12]. Eventually the merosomes rupture and release merozoites, which then infect erythrocytes [13]. Within the erythrocytes, the parasite either replicates asexually or develops into male or female

1
2
3
4
5
6 gametocytes that can be taken up by the mosquito during a blood meal. After
7
8 fertilization in the mosquito midgut, the newly formed ookinetes transmigrate
9
10 through the midgut epithelium and form cysts under the basal lamina. Within
11
12 these oocysts, sporozoites develop and are liberated into the haemocoel of the
13
14 insect. Sporozoites eventually penetrate the salivary glands of the mosquito,
15
16 ready to be injected into the next vertebrate host.
17
18

19
20 The development of tools for genetic modification of malaria parasites [14] and
21
22 the availability of fluorescent reporter proteins such as GFP and RFP have
23
24 greatly improved the study of the complex interactions of the parasite with cells
25
26 of their hosts [5, 9]. A RedStar-expressing variant of the rodent parasite strain *P.*
27
28 *berghei* has been generated that is very well suited for *in vitro* live imaging of
29
30 the parasite development in hepatoma cell culture lines [8].
31
32

33
34 In 2004, Tsien et al. used directed mutation as well as iterative somatic
35
36 hypermutation to enhance mRFP fluorescence [15, 16]. Some of the resulting
37
38 red fluorescent proteins were reported to be much brighter and more photostable
39
40 than the conventional RFPs dsRed or RedStar [16]. However, these data were
41
42 generated using isolated recombinant fluorescent proteins in solution. To test the
43
44 suitability of these new RFP variants in parasites, we generated transgenic,
45
46 clonal *P. berghei* lines expressing the two most promising candidates, tdTomato
47
48 and mCherry.
49
50
51
52
53
54
55
56
57
58
59
60

2 Material and methods

Generation of transgenic *P. berghei* lines expressing red fluorescent proteins

(RedStar, tdTomato, mCherry): The RedStar-expressing *P. berghei* line has been generated previously and was named *P. berghei*-RFP in a previous publication [8]. Since all parasite lines discussed in the present paper express RFP derivatives we have re-named the parasite line expressing the RFP variant RedStar as *P. berghei*-RedStar. Two additional transgenic *P. berghei* lines expressing other red fluorescent proteins were generated by subcloning the tdTomato and mCherry coding sequences from the supplied pRSET-B plasmids [16]; these sequences were subsequently inserted into the *Plasmodium* expression plasmid pL0017 (www.mr4.org), replacing the GFP coding sequence (Supplementary Figure 1A). All genes encoding fluorescent proteins are under the control of the promoter region of the constitutively expressed *P. berghei* eukaryotic elongation factor 1 alpha (eef1aa). The pL0017 plasmid contains target sequences for integration into the c- or d-ssu-rRNA locus of the genome and the *tgdhfr/ts* selectable marker cassette, which allows selection of transfected parasites using pyrimethamine. Plasmids were transfected into blood stage *P. berghei* wildtype schizonts of the ANKA strain using standard methods for genetic modification of *P. berghei* [17]. After pyrimethamine selection of the transgenic parasites, the parent lines were cloned by injection of single infected detached hepatocytes or merozoites into mice. Briefly, HepG2 cells were

1
2
3
4
5
6 infected with transgenic sporozoites and the resulting detached infected
7
8 hepatocytes were collected 65 hours later. Individual detached cells were
9
10 isolated and injected intravenously into naïve mice. The cloned parasites from
11
12 the resulting blood stage infections were collected and used for further analysis.
13
14 Correct integration of the genes encoding the fluorescent proteins into the
15
16 genome was analyzed by PCR (Supplementary Figure 1B). The two new
17
18 transgenic parasite lines that were generated are referred to as *P. berghei*-
19
20 tdTomato and *P. berghei*-mCherry.
21
22
23

24
25 **Culture of HepG2 cells:** HepG2 cells were obtained from the European cell
26
27 culture collection and cultured in Minimum Essential medium with Earle's salts
28
29 supplemented with 10% FCS, 1% L-glutamine and 1% Penicillin/Streptomycin
30
31 (all purchased from PAA Laboratories, Austria). The cells were kept at 37°C and
32
33 5% CO₂ and were split by trypsinization.
34
35

36
37 **Preparation of *P. berghei* parasites for *in vitro* live imaging:** To analyze liver
38
39 stage parasites, 1x10⁵ HepG2 cells were seeded into glass bottom dishes (WillCo
40
41 Wells BV, The Netherlands). *P. berghei* sporozoites were isolated from salivary
42
43 glands of infected *Anopheles stephensi* mosquitoes 18-25 days after an
44
45 infectious blood meal. Approximately 2x10⁴ sporozoites were added to the
46
47 HepG2 cells and incubated for a period of 2 h. After this period, the sporozoite-
48
49 containing medium was removed and the cells were incubated in fresh culture
50
51 medium at 37°C and 5% CO₂. For photostability experiments, parasites were
52
53 imaged at 48 h post infection as described below. For imaging of the different
54
55
56
57
58
59
60

1
2
3
4
5
6 liver stages, GFP-expressing HepG2 cells were infected, and nuclei were stained
7
8 with 1 $\mu\text{g/ml}$ Hoechst 33342 at different time points after infection as described
9
10 previously [8].

11
12 For imaging of blood stage parasites, a droplet of blood was taken from the tail
13
14 vein of infected female NMRI mice, diluted with PBS and put on a microscope
15
16 slide coated with 0.5 mg/ml concanavalin A. A cover slip was placed on top and
17
18 sealed to the slide to prevent dehydration of the cells. Parasites were then
19
20 imaged as described below.
21
22

23
24 **Preparation of *P. berghei* parasites for intravital imaging:** For imaging of
25
26 liver stages, $4\text{-}8 \times 10^5$ *P. berghei* sporozoites were collected from salivary glands
27
28 of infected *A. stephensi* mosquitoes and injected intravenously into female
29
30 NMRI mice. At 44 h post infection, the mice were anesthetized with
31
32 rompun/xylozine and prepared for imaging of the parasites in the liver as
33
34 described previously [18].
35
36

37
38 For imaging of blood stages, female NMRI mice were infected by
39
40 intraperitoneal injection of blood stage parasites. At a parasitemia of 10-15%,
41
42 the mice were anesthetized and prepared for imaging of the liver as described
43
44 [18], allowing infected erythrocytes adhering near the liver capsule to be
45
46 imaged.
47
48

49
50 **Preparation of *P. berghei* parasites for imaging of fixed samples:** 1×10^5

51
52 HepG2 cells were seeded on cover slips in 24 well plates. The cells were
53
54 infected with *P. berghei* sporozoites as described for *in vitro* live imaging. At 48
55
56

1
2
3
4
5
6 h post infection, the culture medium was removed and the cells were fixed in 4%
7
8 paraformaldehyde for 20 minutes. They were washed three times with PBS and
9
10 then either directly mounted on microscope slides with Dako Fluorescent
11
12 Mounting Medium (Dako, Cambridgeshire, UK) or additionally incubated with
13
14 methanol for 10 minutes. The methanol-treated cells were again washed three
15
16 times with PBS and then mounted on slides.
17
18

19
20 **Wide-field imaging:** Wide-field microscopy was performed with a Zeiss
21
22 Observer.Z1 inverted microscope. A Zeiss 63x Plan-Apochromat 1.4 Oil
23
24 objective was used and images were acquired with the Zeiss Axiovision software
25
26 version 4.6. Fluorescence was excited by a Kuebler Codix HXP120 lamp
27
28 (Leistungselektronik Jena, Germany) in combination with the Zeiss filter set 43
29
30 (1114-101), which passed the emitted light through a 605/70 nm bandpass filter
31
32 before detection via a QuantEM:512SC EMCCD camera (Spectra Services,
33
34 USA). During image collection, cells were kept in a CO₂ incubator at 37°C and
35
36 mice were placed on a heating platform in order to maintain their body
37
38 temperature under anesthesia.
39
40
41
42

43
44 **Confocal imaging:** For brightness and photostability experiments, confocal
45
46 microscopy was performed with a Zeiss Observer.Z1 inverted microscope in an
47
48 LSM 5 Live imaging setup. A Zeiss 63x Plan-Apochromat 1.4 Oil objective was
49
50 used and images were acquired with the Zeiss Efficient Navigation 2008
51
52 software. Red fluorescence was excited by a CompassTM 561nm 40mW diode
53
54 pumped laser (Coherent, USA) and emission light passed through a 575 nm
55
56
57
58
59
60

1
2
3
4
5
6 longpass filter before detection via a CCD line detector. The master gain was set
7
8 to 30 and the pinhole to 1 Airy unit. During imaging, cells were kept in a CO₂
9
10 incubator at 37°C and mice were placed on a heating platform in order to
11
12 maintain their body temperature under anesthesia.

13
14 Images of liver stage parasites were acquired with an Olympus IX81 microscope
15
16 in a confocal laser scanning setup. An Olympus 60x Plan-Apochromat 1.35 Oil
17
18 objective was used and images were acquired with the Olympus Fluoview
19
20 software version 1.7b. Fluorescence was excited by a 405 nm diode laser
21
22 (Olympus, Germany), a 488 nm argon laser (Olympus, Germany) and a 559 nm
23
24 diode laser (NTT Electronics, USA) and emission light passed through a
25
26 405/Mar/5437635 filter set before detection. Cells were kept in a CO₂ incubator
27
28 at 37°C.
29
30
31
32
33

34 **Determination of mean fluorescence intensity and photostability:** Infected
35
36 cells were exposed to 90 seconds of constant wide-field or confocal illumination.
37
38 Every two seconds the mean red fluorescence intensity of the parasite was
39
40 measured in Grey for wide-field imaging and on a 256-grey scale for confocal
41
42 imaging. The initial mean fluorescence intensity was set to 100% and the drop in
43
44 intensity was calculated in relation to this value. For *in vitro* live imaging, 15 to
45
46 22 parasites of each *P. berghei* strain were examined; for intravital imaging, 3 to
47
48 6 parasites were analyzed.
49
50
51
52

53 **Imaging of *P. berghei*-RedStar and -mCherry parasites in mosquito stages:**
54
55 Parasites in midguts (oocyst stage) and salivary glands (sporozoite stage) of
56
57
58
59
60

1
2
3
4
5
6
7
8
9
10
11
12
13
14
15
16
17
18
19
20
21
22
23
24
25
26
27
28
29
30
31
32
33
34
35
36
37
38
39
40
41
42
43
44
45
46
47
48
49
50
51
52
53
54
55
56
57
58
59
60

infected mosquitoes were either imaged in the intact mosquito or in PBS after dissection of the midgut or the salivary glands. Images were acquired in the wide-field microscopy setup described above.

Data analysis: Statistical analysis was performed with the Prism software version 4.0a using the two-tailed unpaired t test. Curve fits were also carried out with the Prism software.

3 Results

Since our research is mainly focused on the interactions of the malaria parasite with its host during its development in the liver, most of the imaging analyses presented concentrate on liver stage parasites. However, corresponding experiments have been performed for blood stage parasites (Supplementary Tables 1 and 2).

We used *P. berghei* parasites constitutively expressing RedStar to analyze parasite development in liver cells by confocal laser scanning microscopy (Figure 1A). Clearly, *P. berghei*-RedStar parasites show bright fluorescence in *in vitro* live imaging experiments. In contrast, imaging of these parasites within the livers of living animals resulted in rapid bleaching (Figure 1B). After only 90 seconds of exposure to 3% laser intensity, the RedStar parasites were hardly detectable. To analyze the dynamics of host-parasite interactions *in vivo*, for example the interaction between infected hepatocytes and host immune cells, long exposure times are a prerequisite and thus *P. berghei*-RedStar parasites are

1
2
3
4
5
6 not suitable for such experiments. Therefore, we tested two alternative red
7
8 fluorescent proteins for the expression in murine malaria parasites. These
9
10 proteins, tdTomato and mCherry, have been reported to show bright
11
12 fluorescence and enhanced photostability [16].
13

14
15 We generated two clonal transgenic *P. berghei* lines (*P. berghei*-tdTomato and
16
17 *P. berghei*-mCherry; Supplementary Figure 1), which carry the coding
18
19 sequences of these reporter proteins integrated into the genome. Human
20
21 hepatoma cells were infected with *P. berghei*-RedStar, -tdTomato and -mCherry
22
23 sporozoites, and parasites were imaged by confocal laser scanning microscopy at
24
25 48 h post infection using a laser intensity of 0.5% (Figure 2A, upper panel).
26
27 tdTomato and mCherry parasites are clearly much brighter than RedStar
28
29 parasites. When imaged at a laser intensity of 3%, which is optimal for *P.*
30
31 *berghei*-RedStar, tdTomato and mCherry parasites are drastically overexposed
32
33 (Figure 2A, lower panel). Because of the profound difference in fluorescence
34
35 intensity of the parasites from the different transgenic lines, it was not possible
36
37 to perform photostability measurements always under the same settings (laser
38
39 intensity, exposure time) for all three lines. The details of the settings are
40
41 provided in Figure 2B and in Supplementary Table 1. Comparison of absolute
42
43 fluorescence measured in mean fluorescence intensity (MFI) revealed that
44
45 tdTomato and mCherry are significantly brighter even when imaged at a lower
46
47 laser intensity than RedStar expressing parasites (Figure 2B).
48
49
50
51
52
53
54
55
56
57
58
59
60

1
2
3
4
5
6 For determination of the photostability during intravital imaging of the parasite
7 liver stage, NMRI mice were injected intravenously with *P. berghei* sporozoites
8 of the respective parasite lines. At 44 h post infection, the livers of these mice
9 were surgically exposed for analysis by intravital microscopy. Comparable to the
10 results obtained during *in vitro* live imaging, *P. berghei*-RedStar parasites were
11 less bright than parasites of the *P. berghei*-tdTomato and -mCherry lines and
12 thus a higher laser intensity was needed to achieve similar fluorescence
13 intensities (Figure 3, Supplementary Table 2). Upon illumination, a subset of
14 bright *P. berghei*-RedStar parasites initially bleach rapidly but a low level of
15 fluorescence remains that is then lost at a much slower rate (Figure 3, first
16 panel). A similar bleaching behavior has been described previously for tagRFP,
17 a red fluorescent protein derived from *Entacmaea quadricolor* [19]. Most of the
18 observed *P. berghei*-RedStar parasites, however, did not clearly show this rapid
19 biphasic bleaching. Their absolute fluorescence intensity (on a 256-grey scale)
20 was already weak at the beginning of the experiment, either due to variation of
21 expression levels or their location in different focal planes (Supplementary
22 Figure 2). For these parasites, the drop in fluorescence was comparatively low.
23
24
25
26
27
28
29
30
31
32
33
34
35
36
37
38
39
40
41
42
43
44
45
46
47
48
49
50
51
52
53
54
55
56
57
58
59
60

Whatever the explanation for the different fluorescence intensity and bleaching behavior of this RFP derivative is, it is clear that *P. berghei*-RedStar parasites are not suitable for intravital imaging experiments lasting for several hours.

Although tdTomato has been reported to have enhanced photostability, *P. berghei*-tdTomato parasites bleached equally as fast as RedStar parasites in

1
2
3
4
5
6 intravital imaging experiments. After 90 seconds of illumination, nearly 50% of
7
8 the initial fluorescence intensity was lost (Figure 3, second panel). Moreover, the
9
10 parasites observed in the liver of the infected mouse had a low fluorescence
11
12 intensity even at the beginning of illumination. In contrast to *P. berghei*-RedStar
13
14 and -tdTomato, *P. berghei*-mCherry parasites were bright and hardly bleached
15
16 over the course of the experiment. After 90 seconds of illumination, more than
17
18 90% (91±2%) of the initial fluorescence intensity still remained (Figure 3, third
19
20 panel).
21
22
23

24
25 All photostability data obtained for liver and blood stage parasites are
26
27 summarized in Figure 4. For confocal imaging (Figure 4A), it can be concluded
28
29 that mCherry is by far the best option for the analysis of liver and blood stage
30
31 parasites by *in vitro* live imaging and for the analysis of liver stage parasites by
32
33 intravital imaging. In contrast to the clear difference in bleaching between liver
34
35 stages of *P. berghei*-RedStar and *P. berghei*-mCherry, intravital imaging of the
36
37 blood stages of these parasites showed comparable bleaching features of for both
38
39 RFP derivatives. However, since mCherry is much brighter than RedStar (Figure
40
41 2B and Supplementary Table 2), it is also the protein of choice for the intravital
42
43 analysis of parasites in red blood cells. The jags in the individual bleaching
44
45 curves of the blood stages (Figure 4, on the right) result from the small size of
46
47 the parasites. Even a slight movement of the anesthetized animal causes a shift
48
49 of the infected red blood cell out of the focal plane, which in turn results in a
50
51 drop in recorded fluorescence. Still, the curves allow for an estimation of the
52
53
54
55
56
57
58
59
60

1
2
3
4
5
6 bleaching behavior of the fluorescent proteins expressed by the blood stage
7
8 parasites analyzed in the living host.

9
10 The results for wide-field *in vitro* live imaging experiments (Figure 4B, upper
11 panels) confirm our earlier observations that under *in vitro* conditions, RedStar
12 is rather photostable [8]. In contrast, intravital imaging of infected liver cells
13 showed a rapid bleaching of RedStar and tdTomato even with the less
14 phototoxic wide-field illumination. In comparison with these proteins, mCherry
15 demonstrated enhanced photostability in intravital liver stage imaging (Figure
16 4B lower panel, left). Interestingly, bleaching of tdTomato and RedStar in blood
17 stage parasites was much less evident in wide-field intravital microscopy (Figure
18 4B lower panel, right). However, the absolute fluorescence levels again argue
19 for mCherry as the red fluorescent protein of choice (Supplementary Table 1).

20
21
22
23
24
25
26
27
28
29
30
31
32
33
34 Even after fixation of HepG2 cells infected with fluorescent *P. berghei* parasites,
35 mCherry turned out to be more photostable than RedStar when exposed to laser
36 illumination (Supplementary figure 3). Fixation of RedStar parasites caused a
37 marked decrease in absolute fluorescence (Supplementary figure 3A) and
38 enhanced susceptibility to bleaching (Supplementary figure 3B). In comparison
39 to this, mCherry did not show any loss of fluorescence after PFA fixation
40 (Supplementary figure 3A) and bleached only moderately (Supplementary figure
41 3B).

42 43 44 45 46 47 48 49 50 51 52 53 **4 Discussion**

1
2
3
4
5
6 Our observations of the photostability of all three RFP proteins show that in
7
8 general, they bleach far more rapidly in intravital than in *in vitro* live imaging
9
10 (Figure 4). The process of bleaching is a poorly understood phenomenon, and
11
12 we can therefore only speculate about the reasons for the difference in
13
14 photostability between the fluorescent proteins expressed by liver and blood
15
16 stage parasites. It is assumed that bleaching is related to the formation of an
17
18 excited triplet state of the chromophore upon illumination. This excited triplet
19
20 state can either return to the ground state for another round of excitation or react
21
22 with other molecules. Such reactions can lead to the covalent modification of the
23
24 chromophore and therefore the permanent loss of its ability to fluoresce
25
26 ([http://www.olympusmicro.com/primer/java/fluorescence/photobleaching/index.](http://www.olympusmicro.com/primer/java/fluorescence/photobleaching/index.html)
27
28 [html](http://www.olympusmicro.com/primer/java/fluorescence/photobleaching/index.html)). A prime candidate for such highly reactive molecules would be oxygen
29
30 since it is often present in a natural triplet state. It has been shown that
31
32 fluorescent dyes containing aromatic carbon rings bleach in the presence of
33
34 oxygen [20], and since the chromophores of the red fluorescent proteins have
35
36 such rings, loss of fluorescence in a similar manner is feasible. Oxygen is far
37
38 more readily available as a reaction partner within tissues than in cell culture. In
39
40 most laboratory cultures of mammalian cells such as the HepG2 hepatoma line,
41
42 oxygen reaches the cells by passive diffusion through the culture medium. This
43
44 diffusion process becomes less efficient with increasing fluid levels and a level
45
46 of about 1 mm allows for an optimal oxygen supply for HepG2 cells [21]. In our
47
48 *in vitro* experimental setup, the level of culture medium in the culture dish was
49
50
51
52
53
54
55
56
57
58
59
60

1
2
3
4
5
6 approximately 8 mm. The oxygen supply within the cells was therefore likely
7
8 low. In contrast, within the liver tissue, oxygen should be relatively freely
9
10 available due to distribution via hemoglobin. It is therefore possible that the
11
12 differing photostability observed could be a consequence of the disparity in
13
14 oxygen levels in cell culture and tissue. This might also explain the observation
15
16 that bleaching is usually more pronounced in confocal than in wide-field
17
18 imaging. In the former, the light source is a laser, and it is possible that this
19
20 focused, high-energy excitation allows formation of the triplet state more often
21
22 than does wide-field excitation. An additional aspect that could influence
23
24 bleaching is that in confocal imaging, only light from the focal plane is detected
25
26 and bleaching is therefore immediately obvious. In wide-field imaging, in
27
28 comparison, some degree of bleaching might initially be masked by fluorescence
29
30 from other focal planes.
31
32
33
34

35
36 Another mechanism that could lead to a loss of fluorescence is closely related:
37
38 upon interaction of oxygen with the chromophore triplet state, highly reactive
39
40 singlet oxygen is formed. It will rapidly oxidize molecules containing carbon-
41
42 carbon double bonds [22] and has been shown to damage cells [23, 24].
43
44 However, the detrimental effects of this process are fairly long term and it is thus
45
46 unlikely to play a role during the observation time of 90 seconds used in the
47
48 present study.
49
50
51

52
53 The question remains why we observe a significantly more rapid bleaching for
54
55 RedStar and tdTomato than for mCherry. Various mutations were introduced
56
57
58
59
60

1
2
3
4
5
6 into both tdTomato and mCherry that lead to pronounced changes in
7
8 chromophore architecture. Little is known about the resulting three-dimensional
9
10 structure of tdTomato, but in mCherry the chromophore is distinctly distorted in
11
12 comparison to the planar architecture of mRFP [25]. It is likely that this can lead
13
14 to a different electron density distribution and it is conceivable that this, along
15
16 with steric changes, might hinder the ability of the chromophore to react with
17
18 triplet oxygen or other molecules.
19

20
21
22 Comparisons of the brightness and the bleaching features of red fluorescent
23
24 protein variants are rarely reported in the literature. The few reports discussing
25
26 this topic deal with different sets of fluorescent proteins than used for the present
27
28 study and thus cannot be compared directly. However, the published data
29
30 suggest that the behavior of fluorescent proteins depends on the experimental
31
32 setup and that it is sometimes difficult to predict which RFP variant is suitable
33
34 for expression and imaging in different organisms. It is therefore worthwhile to
35
36 briefly discuss the previous findings concerning the use of different RFP
37
38 variants. In these studies, the difference in brightness between tdTomato,
39
40 mCherry and dsRed [16] has been analysed but not that of RedStar. RedStar is
41
42 reported to be twenty times brighter than dsRed [4], but this is based on
43
44 measurements in bacterial and yeast expression systems, which might differ
45
46 from expression in parasites or mammalian cells. Since mCherry showed a
47
48 reduced brightness compared to dsRed [16], it is surprising that mCherry
49
50 expressed in *P. berghei* is even brighter than RedStar. One possible explanation
51
52
53
54
55
56
57
58
59
60

1
2
3
4
5
6 could be that the data of Shaner et al. were obtained using a Xenon arc lamp for
7
8 excitation of the proteins whereas we used either a HXP120 lamp or laser
9
10 excitation. For confocal imaging of RFP expressing parasites, we used a laser
11
12 excitation wavelength of 561 nm, and thus not all RFP derivatives will be excited
13
14 equally well. However, RedStar and tdTomato with excitation maxima at 558
15
16 and 554 nm, respectively are closer to the excitation wavelength of the laser than
17
18 mCherry with an excitation maximum of 587 nm. Therefore the fixed excitation
19
20 wavelength of the laser cannot be the reason for the superior brightness of
21
22 mCherry. Another, more likely explanation is that while mCherry is already
23
24 fluorescent as a monomer, RedStar and dsRed have to reach a tetrameric state
25
26 before they can emit fluorescence. It is therefore possible that the tetrameric
27
28 conformation is not achieved equally well upon expression in different
29
30 organisms. A similar effect would also explain why in our experiments
31
32 tdTomato is not, as published, five times brighter than mCherry [16]. tdTomato,
33
34 unlike the monomeric mCherry, is a linked dimer, and therefore the correct
35
36 folding of the protein could be more problematic.
37
38
39
40
41
42
43
44
45

46 **5 Concluding remarks**

47
48 In comparison to RedStar and tdTomato, mCherry is the protein of choice for the
49
50 analysis of *Plasmodium* liver and blood stages by confocal and wide-field *in*
51
52 *vivo* imaging. It generally shows the brightest fluorescence and, more
53
54 importantly, proves to be far more photostable. This is most impressively
55
56
57
58
59
60

1
2
3
4
5
6 demonstrated during the analysis of the liver stages of the parasite by intravital
7
8 microscopy. mCherry has recently also been recommended for tomographic
9
10 imaging where red fluorescent proteins are preferentially used because they emit
11
12 at wavelengths where tissue absorption is low [26]. Moreover, mCherry is
13
14 convenient also in the mosquito stages of *P. berghei* because it makes analysis
15
16 and selection of infected mosquitoes under a fluorescence binocular easier
17
18 (Supplementary Figure 3).
19
20
21
22
23
24
25
26

27 **Acknowledgments**

28
29 We would like to thank Roger Y. Tsien (Howard Hughes Medical Institute,
30
31 University of California at San Diego, La Jolla, CA) for his kind gift of
32
33 tdTomato and mCherry plasmids. We are grateful to Rebecca R. Stanway and
34
35 Kathleen E. Rankin for critically reading the manuscript. This work was
36
37 supported by a DFG grant to VH (HE 4497/1-2).
38
39
40
41
42

43 *The authors have declared no conflict of interest.*
44
45
46
47

48 **5 References**

- 49
50
51 [1] Chalfie, M., Tu, Y., Euskirchen, G., Ward, W. W., Prasher, D. C., Green
52
53 fluorescent protein as a marker for gene expression. *Science* 1994, 263, 802-805.
54
55 [2] Matz, M. V., Fradkov, A. F., Labas, Y. A., Savitsky, A. P., *et al.*, Fluorescent
56
57 proteins from nonbioluminescent Anthozoa species. *Nat Biotechnol* 1999, 17,
58
59 969-973.
60

- 1
2
3
4
5
6 [3] Campbell, R. E., Tour, O., Palmer, A. E., Steinbach, P. A., *et al.*, A
7 monomeric red fluorescent protein. *Proc Natl Acad Sci U S A* 2002, *99*, 7877-
8 7882.
- 9 [4] Knop, M., Barr, F., Riedel, C. G., Heckel, T., Reichel, C., Improved version
10 of the red fluorescent protein (drFP583/DsRed/RFP). *Biotechniques* 2002, *33*,
11 592, 594, 596-598 passim.
- 12 [5] Frevert, U., Engelmann, S., Zougbede, S., Stange, J., *et al.*, Intravital
13 observation of Plasmodium berghei sporozoite infection of the liver. *PLoS Biol*
14 2005, *3*, e192.
- 15 [6] Amino, R., Menard, R., Frischknecht, F., *In vivo* imaging of malaria
16 parasites--recent advances and future directions. *Curr Opin Microbiol* 2005, *8*,
17 407-414.
- 18 [7] Heussler, V., Doerig, C., *In vivo* imaging enters parasitology. *Trends*
19 *Parasitol* 2006, *22*, 192-195; discussion 195-196.
- 20 [8] Sturm, A., Graewe, S., Franke-Fayard, B., Retzlaff, S., *et al.*, Alteration of
21 the Parasite Plasma Membrane and the Parasitophorous Vacuole Membrane
22 during Exo-Erythrocytic Development of Malaria Parasites. *Protist* 2008.
- 23 [9] Amino, R., Thiberge, S., Shorte, S., Frischknecht, F., Menard, R.,
24 Quantitative imaging of Plasmodium sporozoites in the mammalian host. *C R*
25 *Biol* 2006, *329*, 858-862.
- 26 [10] Amino, R., Thiberge, S., Martin, B., Celli, S., *et al.*, Quantitative imaging of
27 Plasmodium transmission from mosquito to mammal. *Nat Med* 2006, *12*, 220-
28 224.
- 29 [11] Sturm, A., Amino, R., van de Sand, C., Regen, T., *et al.*, Manipulation of
30 host hepatocytes by the malaria parasite for delivery into liver sinusoids. *Science*
31 2006, *313*, 1287-1290.
- 32 [12] Sturm, A., Heussler, V., Live and let die: manipulation of host hepatocytes
33 by exoerythrocytic Plasmodium parasites. *Med Microbiol Immunol* 2007, *196*,
34 127-133.
- 35 [13] Baer, K., Klotz, C., Kappe, S. H., Schnieder, T., Frevert, U., Release of
36 hepatic Plasmodium yoelii merozoites into the pulmonary microvasculature.
37 *PLoS Pathog* 2007, *3*, e171.
- 38 [14] Janse, C. J., Franke-Fayard, B., Mair, G. R., Ramesar, J., *et al.*, High
39 efficiency transfection of Plasmodium berghei facilitates novel selection
40 procedures. *Mol Biochem Parasitol* 2006, *145*, 60-70.
- 41 [15] Wang, L., Jackson, W. C., Steinbach, P. A., Tsien, R. Y., Evolution of new
42 nonantibody proteins via iterative somatic hypermutation. *Proc Natl Acad Sci U*
43 *S A* 2004, *101*, 16745-16749.
- 44 [16] Shaner, N. C., Campbell, R. E., Steinbach, P. A., Giepmans, B. N., *et al.*,
45 Improved monomeric red, orange and yellow fluorescent proteins derived from
46 *Discosoma* sp. red fluorescent protein. *Nat Biotechnol* 2004, *22*, 1567-1572.
- 47 [17] Janse, C. J., Ramesar, J., Waters, A. P., High-efficiency transfection and
48 drug selection of genetically transformed blood stages of the rodent malaria
49 parasite Plasmodium berghei. *Nat Protoc* 2006, *1*, 346-356.
- 50
51
52
53
54
55
56
57
58
59
60

- 1
2
3
4
5
6 [18] Thiberge, S., Blazquez, S., Baldacci, P., Renaud, O., *et al.*, *In vivo* imaging
7 of malaria parasites in the murine liver. *Nat Protoc* 2007, 2, 1811-1818.
8 [19] Merzlyak, E. M., Goedhart, J., Shcherbo, D., Bulina, M. E., *et al.*, Bright
9 monomeric red fluorescent protein with an extended fluorescence lifetime. *Nat*
10 *Methods* 2007, 4, 555-557.
11 [20] Renn, A., Seelig, J., Sandoghdar, V., Oxygen-dependent photochemistry of
12 fluorescent dyes studied at the single molecule level. *Molecular Physics* 2006,
13 *104*, 409-414.
14 [21] Camp, J. P., Capitano, A. T., Induction of zone-like liver function gradients
15 in HepG2 cells by varying culture medium height. *Biotechnol Prog* 2007, 23,
16 1485-1491.
17 [22] Flors, C., Fryer, M. J., Waring, J., Reeder, B., *et al.*, Imaging the production
18 of singlet oxygen *in vivo* using a new fluorescent sensor, Singlet Oxygen Sensor
19 Green. *J Exp Bot* 2006, 57, 1725-1734.
20 [23] Kochevar, I. E., Lynch, M. C., Zhuang, S., Lambert, C. R., Singlet oxygen,
21 but not oxidizing radicals, induces apoptosis in HL-60 cells. *Photochem*
22 *Photobiol* 2000, 72, 548-553.
23 [24] Yang, J. L., Wang, L. C., Chang, C. Y., Liu, T. Y., Singlet oxygen is the
24 major species participating in the induction of DNA strand breakage and 8-
25 hydroxydeoxyguanosine adduct by lead acetate. *Environ Mol Mutagen* 1999, 33,
26 194-201.
27 [25] Shu, X., Shaner, N. C., Yarbrough, C. A., Tsien, R. Y., Remington, S. J.,
28 Novel chromophores and buried charges control color in mFruits. *Biochemistry*
29 2006, 45, 9639-9647.
30 [26] Deliolanis, N. C., Kasmieh, R., Wurdinger, T., Tannous, B. A., *et al.*,
31 Performance of the red-shifted fluorescent proteins in deep-tissue molecular
32 imaging applications. *J Biomed Opt* 2008, 13, 044008.
33
34
35
36
37
38
39
40

41 Figure legends

42
43
44 **Figure 1: *P. berghei*-RedStar is well suited for *in vitro* live imaging but not**
45 **intravital imaging of parasite liver stages.**
46

47 **A** HepG2-GFP cells (green) were infected with *P. berghei*-RedStar sporozoites.
48
49 At the indicated time points after infection, nuclei were stained with Hoechst
50 33342 (blue) and the cells were imaged with a confocal laser-scanning
51 microscope. The parasite (red) progresses from a sporozoite (6 hours post
52
53
54
55
56
57
58
59
60

1
2
3
4
5
6 infection, hpi) to a large schizont (48 hpi) before it divides into merozoites (54
7
8 hpi); eventually the infected hepatocyte detaches (65 hpi).

9
10 **B** An NMRI mouse was infected with 5×10^5 *P. berghei*-RedStar sporozoites by
11
12 intravenous injection. At 44 hours post infection, a liver lobe was surgically
13
14 exposed and parasites (red) were imaged with a confocal laser scanning
15
16 microscope. Bars = 10 μ m
17

18
19
20
21
22 **Figure 2: In confocal imaging of fluorescent *Plasmodium* liver stage**
23
24 **parasites, tdTomato and mCherry are much brighter than RedStar.**

25
26 HepG2 cells were infected with *P. berghei*-RedStar, -tdTomato and -mCherry
27
28 sporozoites, respectively. At 48 hours post infection, parasites were imaged by
29
30 confocal laser scanning microscopy at different laser intensities.
31
32

33
34 **A** At the optimal laser intensity for the imaging of tdTomato and mCherry
35
36 (0.5%), RedStar fluorescence is too weak to be clearly detected, while the
37
38 optimal setting for RedStar (3%) results in an overexposure for tdTomato and
39
40 mCherry.
41
42

43
44 Bar = 10 μ m

45
46 **B** Absolute fluorescence levels are compared at optimal laser intensities (LI,
47
48 indicated by the boxed numbers). At low LI (0.5%), mCherry is significantly
49
50 brighter than that of tdTomato (LI 0.5%) and RedStar at higher LI (3%). n=15,
51
52
53 ** = $p < 0.005$, *** = $p < 0.0001$.
54
55
56
57
58
59
60

1
2
3
4
5
6 **Figure 3: In intravital imaging of *Plasmodium* liver stage parasites,**
7 **mCherry is far more photostable than RedStar and tdTomato.**
8

9
10 NMRI mice were injected intravenously with *P. berghei* sporozoites of the
11 respective parasite lines. At 44 hours post infection, the liver was surgically
12 exposed and parasites were imaged by confocal laser scanning microscopy. The
13 mean fluorescence intensity was measured every two seconds during a 90
14 second period of constant illumination optimal for image acquisition for the
15 respective red fluorescent protein. The images presented were acquired at the
16 beginning (0 sec) and at the end (90 sec) of the photostability assay. The drops
17 in mean fluorescence intensity were calculated in relation to the initial intensity
18 and are indicated in the graphs (mean and the standard deviation of several cells
19 imaged per experiment are presented). A curve fit was performed (shown as a
20 thin black line) and the bleaching of RedStar and tdTomato was found to fit best
21 a biphasic exponential decay curve ($R^2=0.9906$ and $R^2=0.9978$, respectively).
22 Bars = 10 μ m. Total numbers of recorded parasites are shown in Supplementary
23 table 1.
24
25
26
27
28
29
30
31
32
33
34
35
36
37
38
39
40
41
42
43
44
45

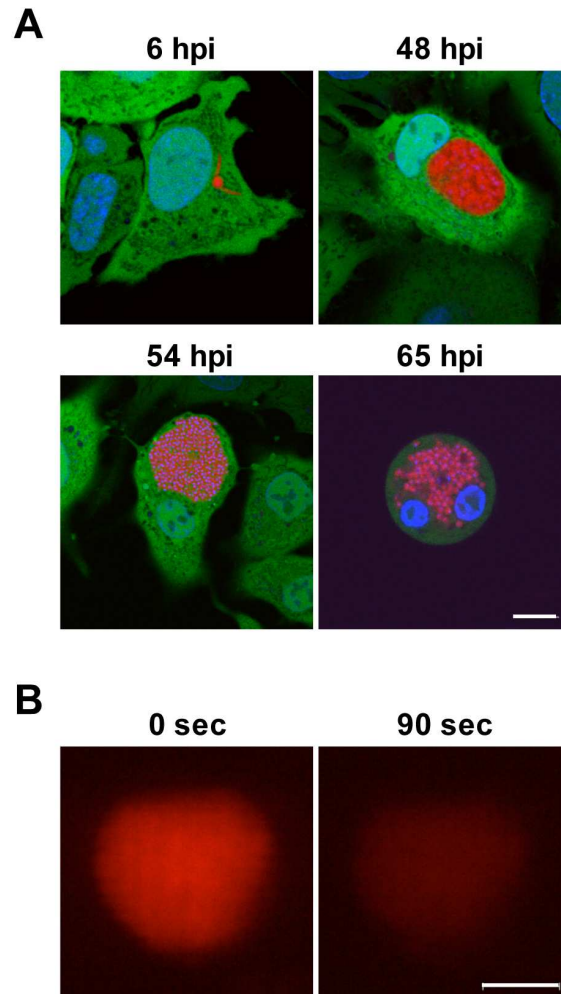
46 **Figure 4: Of the red fluorescent parasite strains tested, *P. berghei*-mCherry**
47 **is best suited for live imaging.**
48

49
50 *P. berghei*-RedStar, -tdTomato and -mCherry blood and liver stage parasites
51 were prepared for *in vitro* live imaging and intravital imaging (for details see
52 material and methods section). Individual fluorescent parasites were exposed to
53
54
55
56
57
58
59
60

1
2
3
4
5
6 90 seconds of constant confocal laser scanning (A) or wide-field (B)
7
8 illumination and the mean red fluorescence was measured every two seconds.
9
10 The drop in fluorescence intensity is shown as the percentage of the initial mean
11
12 fluorescence for individual parasites. Total numbers of recorded parasites are
13
14 shown in supplementary table 1.
15
16
17
18
19
20
21
22
23
24
25
26
27
28
29
30
31
32
33
34
35
36
37
38
39
40
41
42
43
44
45
46
47
48
49
50
51
52
53
54
55
56
57
58
59
60

For Peer Review

Figure 1: Graewe et al



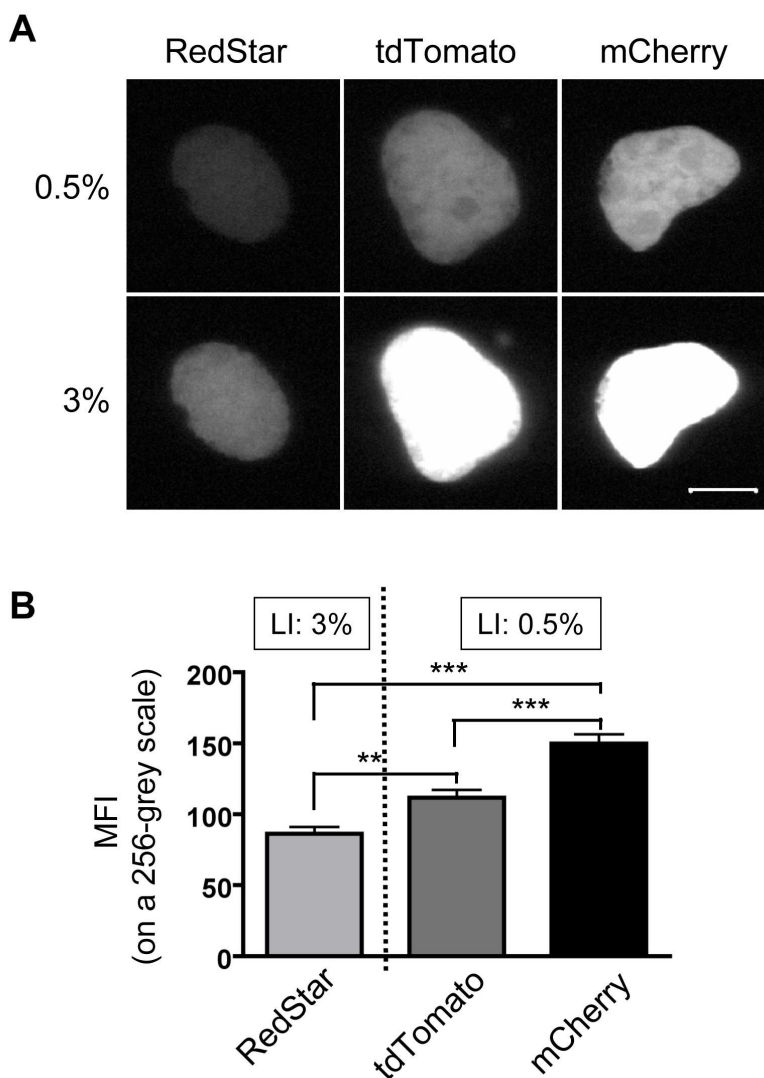
P. berghei-RedStar is well suited for in vitro live imaging but not intravital imaging of parasite liver stages.

A HepG2-GFP cells (green) were infected with P. berghei-RedStar sporozoites. At the indicated time points after infection, nuclei were stained with Hoechst 33342 (blue) and the cells were imaged with a confocal laser-scanning microscope. The parasite (red) progresses from a sporozoite (6 hours post infection, hpi) to a large schizont (48 hpi) before it divides into merozoites (54 hpi); eventually the infected hepatocyte detaches (65 hpi).

B An NMRI mouse was infected with 5×10^5 P. berghei-RedStar sporozoites by intravenous injection. At 44 hours post infection, a liver lobe was surgically exposed and parasites (red) were imaged with a confocal laser scanning microscope. Bars = 10 μ m

93x165mm (300 x 300 DPI)

Figure 2: Graewe et al



In confocal imaging of fluorescent *Plasmodium* liver stage parasites, tdTomato and mCherry are much brighter than RedStar.

HepG2 cells were infected with *P. berghei*-RedStar, -tdTomato and -mCherry sporozoites, respectively. At 48 hours post infection, parasites were imaged by confocal laser scanning microscopy at different laser intensities.

A At the optimal laser intensity for the imaging of tdTomato and mCherry (0.5%), RedStar fluorescence is too weak to be clearly detected, while the optimal setting for RedStar (3%) results in an overexposure for tdTomato and mCherry.

Bar = 10 μ m

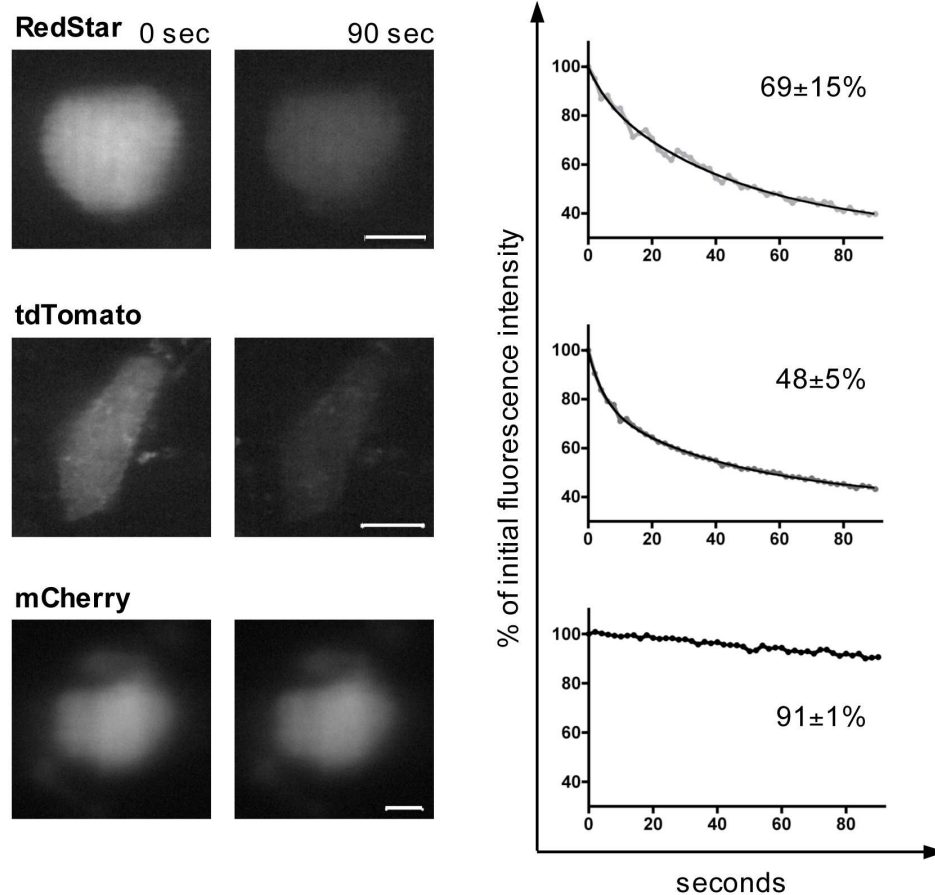
B Absolute fluorescence levels are compared at optimal laser intensities (LI, indicated by the boxed numbers). At low LI (0.5%), mCherry is significantly brighter than that of tdTomato (LI 0.5%) and RedStar at higher LI (3%). n=15, ** = p<0.005, *** = p<0.0001.

1
2
3
4
5
6
7
8
9
10
11
12
13
14
15
16
17
18
19
20
21
22
23
24
25
26
27
28
29
30
31
32
33
34
35
36
37
38
39
40
41
42
43
44
45
46
47
48
49
50
51
52
53
54
55
56
57
58
59
60

139x202mm (300 x 300 DPI)

For Peer Review

Figure 3: Graewe et al



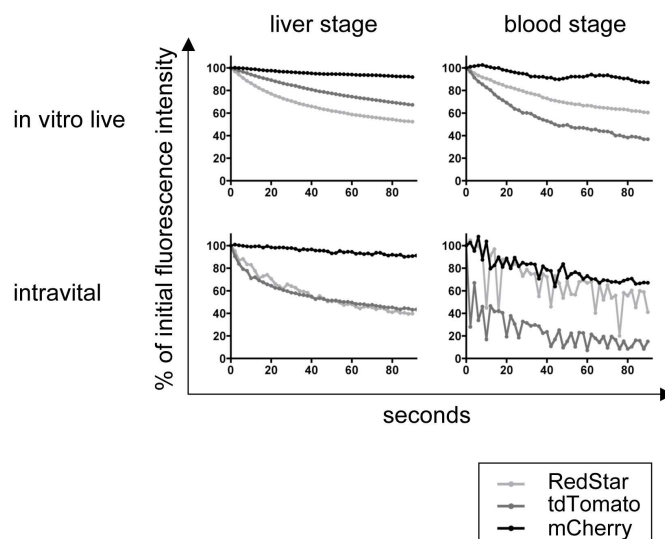
In intravital imaging of Plasmodium liver stage parasites, mCherry is far more photostable than RedStar and tdTomato.

NMRI mice were injected intravenously with *P. berghei* sporozoites of the respective parasite lines. At 44 hours post infection, the liver was surgically exposed and parasites were imaged by confocal laser scanning microscopy. The mean fluorescence intensity was measured every two seconds during a 90 second period of constant illumination optimal for image acquisition for the respective red fluorescent protein. The images presented were acquired at the beginning (0 sec) and at the end (90 sec) of the photostability assay. The drops in mean fluorescence intensity were calculated in relation to the initial intensity and are indicated in the graphs (mean and the standard deviation of several cells imaged per experiment are presented). A curve fit was performed (shown as a thin black line) and the bleaching of RedStar and tdTomato was found to fit best a biphasic exponential decay curve ($R^2=0.9906$ and $R^2=0.9978$, respectively). Bars = $10\mu\text{m}$. Total numbers of recorded parasites are shown in Supplementary table 1.

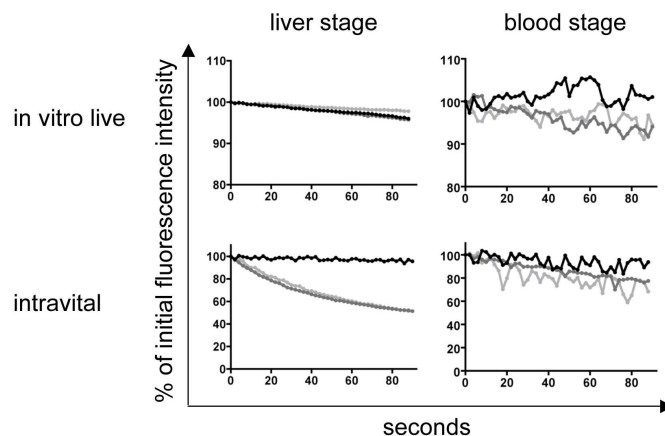
150x160mm (300 x 300 DPI)

Figure 4: Graewe et al

A Confocal



B Wide-Field



Of the red fluorescent parasite strains tested, *P. berghei*-mCherry is best suited for live imaging. *P. berghei*-RedStar, -tdTomato and -mCherry blood and liver stage parasites were prepared for in vitro live imaging and intravital imaging (for details see material and methods section). Individual fluorescent parasites were exposed to 90 seconds of constant confocal laser scanning (A) or wide-field (B) illumination and the mean red fluorescence was measured every two seconds. The drop in fluorescence intensity is shown as the percentage of the initial mean fluorescence for individual parasites. Total numbers of recorded parasites are shown in supplementary table 1.

153x249mm (300 x 300 DPI)